Realization of 2D Spin-orbit Interaction and Exotic Topological Orders in Cold Atoms

Xiong-Jun Liu,[1,2] K. T. Law,[1] and T. K. Ng[1]

[1]*Department of Physics, Hong Kong University of Science and Technology, Clear Water Bay, Hong Kong, China*
[2]*Institute for Advanced Study, Hong Kong University of Science and Technology, Clear Water Bay, Hong Kong, China*

(Dated: April 8, 2013)

Majorana zero bound mode exists in the vortex core of a chiral $p+ip$ superconductor or superfluid, which can be driven from an s-wave pairing state by two-dimensional (2D) spin-orbit (SO) coupling. However, a 2D Rashba-type SO interaction is not experimentally realistic for an atom gas in the continuum. We propose here a novel scheme based on realistic cold atom platforms to generate 2D SO interactions in a blue-detuned square optical lattice, and predict both the quantum anomalous Hall effect and chiral topological superfluid phase in the experimentally accessible parameter regimes. This work opens a new direction with remarkable experimental feasibility to observe non-Abelian topological orders in cold atom systems.

PACS numbers: 37.10.Jk, 71.10.Pm, 42.50.Ex, 71.70.Ej

Introduction.– The search for non-Abelian Majorana fermions has been a focus of both theoretical and experimental studies in condensed matter physics, driven by both the pursuit of exotic fundamental physics and the applications in fault-tolerant topological quantum computation [1–3]. Majorana zero modes (MZMs) are predicted to exist in the vortex core of a two-dimensional (2D) intrinsic $(p+ip)$-wave SC and at the ends of a 1D p-wave SC [1]. Recent studies show that effective 1D and 2D p-wave pairing states can be driven from s-wave SCs by spin-orbit (SO) interactions in the heterostructures formed by conventional s-wave SCs and topological insulators [4] or semiconductors [5, 6], leading to MZMs in the case of odd number of subbands crossing the Fermi level. Following the theoretical prediction, Majorana end states have been suggestively observed in the semiconductor nanowire/s-wave superconductor heterostructures [7] through tunneling transport measurements [8]. However, demonstrating the non-Abelian statistics of MZMs in braiding operation [2], as an unambiguous verification, is a far more demanding task and not yet available in solid-state experiments.

On the other hand, the recent great advancement in realizing synthetic SO coupling in cold atoms [9–14] opens intriguing new avenues to probe topological orders [15–26] with clean platforms in a fully controllable fashion. By far the experimentally realized SO interaction [10–14] is the 1D equal Rashba-Dresselhaus-type SO term through a two-photon Raman process as theoretically proposed in Ref. [9]. Detailed investigations show that only 1D SO term can be realized in an atom gas with internal Λ-type configuration as considered in experiments [9, 27, 28]. With such 1D SO interaction it is unfortunate not optimistic to reach the topological superfluid (SF) phase from an s-wave pairing state in cold atoms. The reason is because on one hand in a quasi-1D system no long-range s-wave order can be obtained; on the other hand, the proximity effect, as used in solid state experiments [7], is not realistic for cold atoms. Therefore, to find out a truly experimental scheme to observe MZMs with higher dimensional SO interactions is a foremost outstanding goal in the current field of cold atoms.

In this letter, we propose a novel scheme to observe both the quantum anomalous Hall effect (QAHE) and chiral topological SF phase with (pseudo)spin-1/2 cold fermions trapped in a blue-detuned square optical lattice and coupled to two periodic Raman fields. The remarkable advantage of our model in the realization is that the square optical lattice and Raman fields, used to induce 2D SO interactions, are generated simultaneously by the same laser fields. Basing our model on real cold atom systems and conventional technologies, we show that the predicted exotic topological orders can be studied with currently available experimental platforms.

Model.–We start with the quasi-2D cold fermions trapped in a conventional square optical lattice, with their internal degree of freedom (atomic spins) experiencing periodic Raman fields $M_{x,y}$ induced by two-photon processes, as illustrated in Fig. 1. The dynamics of fermions are governed by the following Hamiltonian

$$\begin{aligned} H &= \frac{p_x^2}{2m}+\frac{p_y^2}{2m}+V(\mathbf{r})+m_z(|g_\uparrow\rangle\langle g_\uparrow|-|g_\downarrow\rangle\langle g_\downarrow|) \\ &\quad -\big\{\big[M_x(x)+iM_y(y)\big]|g_\uparrow\rangle\langle g_\downarrow|+\text{H.c.}\big\}, \end{aligned} \tag{1}$$

where $M_x = M_0\sin(k_0x)$ and $M_y = M_0\sin(k_0x)$, and the optical dipole potential $V(\mathbf{r}) = -V_0\big[\cos^2(k_0x)+\cos^2(k_0y)\big]$ forms the square lattice. Below we describe how to obtain H with the realistic cold atom platform. The diagram for light-atom couplings is shown in Fig. 1(a). The ground states $|g_{\uparrow,\downarrow}\rangle$ are coupled to the excited one $|e\rangle$ through two pairs of lasers $\Omega_{1,2}$ and $\tilde{\Omega}_{1,2}$, which form two Λ-type configurations with large one-photon blue detunings Δ_1 and Δ_2, respectively. For the present purpose, we set $\Omega_1 = \Omega_0\sin(k_0x)$ and $\Omega_2 = \Omega_0\sin(k_0y)$, while $\tilde{\Omega}_1 = i\tilde{\Omega}_2 = \Omega_0$ to be constants. For the parameter regime that $\Delta_{1,2} \gg |\Delta_1-\Delta_2| \gg$

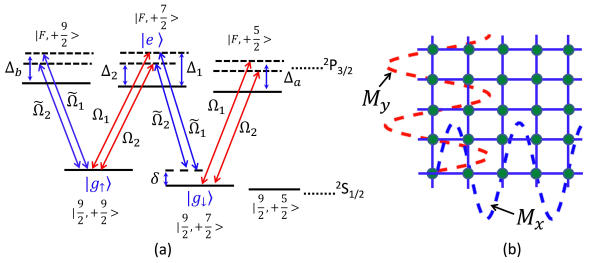

FIG. 1: (Color online) (a) A realistic optical-dipole transition diagram in cold fermions (^{40}K) coupled to two pairs of laser beams $\Omega_{1,2}$ and $\tilde{\Omega}_{1,2}$ under large blue-detuning condition. (b) With this configuration a square lattice potential and two periodic Raman fields $M_{x,y}$ are simultaneously generated.

$|\Omega_0^2/\Delta_{1,2}|$, the population of the excited state $|e\rangle$ is negligible [9] and the light-atom couplings through two detuned Λ-type configurations lead to two independent Raman transitions between $|g_\uparrow\rangle$ and $|g_\downarrow\rangle$, with the Raman fields given by $M_x = \hbar|\Omega_0|^2\sin(k_0x)/\Delta_1$ and $iM_y = i\hbar|\Omega_0|^2\sin(k_0y)/\Delta_2$, respectively [Fig. 1(a)]. Such two Raman processes can be precisely tuned with acousto-optic modulator to have a small two-photon off-resonance δ ($|\delta| \ll |\Omega_0^2/\Delta_{1,2}|$) which gives rise to the Zeeman term $m_z = \hbar\delta/2$ along z axis in H [19]. Finally, note in the realistic atom system, e.g. for the ^{40}K atoms the lasers $\Omega_{1,2}$ ($\tilde{\Omega}_{1,2}$) also couple to the state $|g_\downarrow\rangle$ ($|g_\uparrow\rangle$) with corresponding large detunings $\Delta_{a_{1,2}}$ ($\Delta_{b_{1,2}}$) [see Fig. 1 (a)]. While these additional couplings cannot lead to new Raman transitions between $|g_{\uparrow,\downarrow}\rangle$ and other ground levels due to large two-photon detunings [12, 13], they contribute to the diagonal optical potentials for the two ground states and we get $V_\uparrow = \sum_{j=1,2}(|\Omega_j|^2/\Delta_j + |\tilde{\Omega}_j|^2/\Delta_{b_j})$ and $V_\downarrow = \sum_j(|\tilde{\Omega}_j|^2/\Delta_j + |\Omega_j|^2/\Delta_{a_j})$. In the realistic experiment (e.g. for ^{40}K atoms) the magnitudes of detunings $\Delta_{a,b,j}$ (can be over 10^3GHz) are much larger than their differences (in the order of 10MHz) [12]. Therefore in the formulas of V_σ and $M_{x,y}$ we can take that $\Delta_1 = \Delta_2 = \Delta_{a_{1,2}} = \Delta_{b_{1,2}} = \Delta$, which is followed by $V_\uparrow = V_\downarrow = -(|\Omega_0|^2/\Delta)\big[\cos^2(k_0x) + \cos^2(k_0y)\big] + const.$ and $M_0 = \hbar|\Omega_0|^2/\Delta$. Neglecting the constant terms yields the effective Hamiltonian in Eq. (1). In brief, in Fig. 1 the lasers $\Omega_{1,2}$ (red lines) generate the conventional square lattice. Together with another pair of lasers $\tilde{\Omega}_{1,2}$ the Raman fields are simultaneously created.

Before proceeding further, we provide two important remarks on the realization. First, since the Raman fields and the optical lattice potentials are simultaneously achieved by the same lasers, the phase fluctuations in the lasers, characterized by $\Omega_1 = \Omega_0\sin(k_0x + \phi_1^{\rm fluc})$ and $\Omega_2 = \Omega_0\sin(k_0y + \phi_2^{\rm fluc})$, only lead to global shift of the lattice and Raman fields as illustrated in Fig. 1(b). The relative spatial profile of $M_{x,y}$ and $V(\mathbf{r})$ is always automatically fixed and therefore the effective Hamiltonian (1) is unchanged. This greatly simplifies the experimental set-up and makes the realization of this model is no more difficult than that of a conventional square lattice for spin-1/2 cold fermions. Second, the blue detuning is essential for the realization. If using red-detuned lasers, i.e. $\Delta_{a,b,j} < 0$, one has then $V_{\uparrow,\downarrow} = -(|\Omega_0^2/\Delta|)\big[\sin^2(k_0x) + \sin^2(k_0y)\big]$, which shifts 1/2 lattice site relative to the Raman fields. The red-detuned laser couplings cannot lead to 2D SO interaction or nontrivial topological orders as studied below.

Quantum anomalous Hall effect.—The tight-binding model of H can be derived straightforwardly. We take that fermions occupy the lowest s-orbitals $\phi_{s\sigma}$ ($\sigma =\uparrow,\downarrow$), and consider only the nearest-neighbor hopping terms. The tight-binding Hamiltonian is given by $H_{\rm TI} = -t_s\sum_{<\vec{i},\vec{j}>,\sigma}\hat{c}^\dagger_{\vec{i}\sigma}\hat{c}_{\vec{j}\sigma} + \sum_{\vec{i}} m_z(\hat{n}_{\vec{i}\uparrow} - \hat{n}_{\vec{i}\downarrow}) + \big[\sum_{<\vec{i},\vec{j}>} t_{\rm so}^{\vec{i}\vec{j}}\hat{c}^\dagger_{\vec{i}\uparrow}\hat{c}_{\vec{j}\downarrow} + \text{H.c.}\big]$, where t_s denotes spin-conserved hopping, the 2D lattice-site index $\vec{i} = (i_x, i_y)$, and $\hat{n}_{\vec{i}\sigma} = \hat{c}^\dagger_{\vec{i}\sigma}\hat{c}_{\vec{i}\sigma}$. From the even-parity of the s-orbitals and the profile of Raman fields shown in Fig. 1(b), it can be directly verified that the spin-flip hopping terms due to the Raman fields satisfy $t_{\rm so}^{j_x,j_x\pm1} = \pm(-1)^j t_{\rm so}^{(0)}$ and $t_{\rm so}^{j_y,j_y\pm1} = \pm i(-1)^j t_{\rm so}^{(0)}$, where $t_{\rm so}^{(0)} = M_0\int d^2\vec{r}\phi_s(x,y)\sin(k_0x)\phi_s(x-a,y)$ with a the lattice constant. Redefining the spin-down operator $\hat{c}_{\vec{j}\downarrow} \to e^{i\pi\vec{r}_j/a}\hat{c}_{\vec{j}\downarrow}$, we recast the Hamiltonian into

$$\begin{aligned} H_{\rm TI} = & -t_s\sum_{<\vec{i},\vec{j}>}(\hat{c}^\dagger_{\vec{i}\uparrow}\hat{c}_{\vec{j}\uparrow} - \hat{c}^\dagger_{\vec{i}\downarrow}\hat{c}_{\vec{j}\downarrow}) + \sum_{\vec{i}} m_z(\hat{n}_{\vec{i}\uparrow} - \hat{n}_{\vec{i}\downarrow}) + \\ & + \big[\sum_{j_x} t_{\rm so}^{(0)}(\hat{c}^\dagger_{j_x\uparrow}\hat{c}_{j_x+1\downarrow} - \hat{c}^\dagger_{j_x\uparrow}\hat{c}_{j_x-1\downarrow}) + \text{H.c.}\big] + \\ & + \big[\sum_{j_y} it_{\rm so}^{(0)}(\hat{c}^\dagger_{j_y\uparrow}\hat{c}_{j_y+1\downarrow} - \hat{c}^\dagger_{j_y\uparrow}\hat{c}_{j_y-1\downarrow}) + \text{H.c.}\big]. \quad (2) \end{aligned}$$

It is convenient to rewrite H in the k-space and $H_{\rm TI} = -\sum_{\mathbf{k},\sigma\sigma'}\hat{c}^\dagger_{\mathbf{k},\sigma}[d_z(\mathbf{k})\sigma_z + d_x(\mathbf{k})\sigma_x + d_y(\mathbf{k})\sigma_y]_{\sigma,\sigma'}\hat{c}_{\mathbf{k},\sigma'}$, with $d_x = 2t_{\rm so}^{(0)}\sin(k_ya)$, $d_y = 2t_{\rm so}^{(0)}\sin(k_xa)$ and $d_z = -m_z + 2t_s\cos(k_xa) + 2t_s\cos(k_ya)$. A simple analysis shows that the bulk system is gapped when $|m_z| \neq 4t_s, 0$. By calculating the first Chern number $C_1^{\rm AH} = (4\pi)^{-1}\int d^2\mathbf{k}\cdot\partial_{k_x}\mathbf{n}\times\partial_{k_y}\mathbf{n}$, with $\mathbf{n} = (d_x, d_y, d_z)/|\vec{d}(\mathbf{k})|$, one can verify that the above Hamiltonian describes a topological insulator for $0 < |m_z| < 4t_s$ and otherwise a trivial insulator. This result can be read by analyzing the band structure around the four independent Dirac points at $\mathbf{k}_c = (0,0), (0,\pi), (\pi,0)$, and (π,π), where the system are described by massive Dirac equations. First, it is straightforward to know that the system is a trivial insulator when $m_z \gg 4t_s$. Upon reducing m_z to $m_z = 4t_s$ the band gap closes at $\mathbf{k}_c = (0,0)$ and reopens when $0 < m_z < 4t_s$, with the effective mass at this Dirac point changes sign and leads to the change by 1 in the Chern number. Therefore the system is in the topological phase when $0 < m_z < 4t_s$ with $C_1^{\rm AH} = 1$. In the same way,

one can determine that the phase is also topological for $-4t_s < m_z < 0$. On the other hand, both masses of the Dirac Hamiltonians around $\mathbf{k}_c = (0,\pi)$ and $(\pi,0)$ change sign when varying $m_z < 0$ to $m_z > 0$, implying that $C_1^{\rm AH}(m_z = 0_+) - C_1^{\rm AH}(m_z = 0_-) = 2$ and therefore $C_1^{\rm AH} = -1$ for $-4t_s < m_z < 0$. We then conclude that the Hamiltonian (2) realizes a QAHE with the quantized Hall conductance

$$\sigma_{xy}^{\rm AH} = \begin{cases} \mathrm{sgn}(m_z)\frac{1}{\hbar}, & \text{for } 0 < |m_z| < 4t_s, \\ 0, & \text{for } |m_z| \geq 4t_s, m_z = 0. \end{cases} \quad (3)$$

It is noteworthy that while the QAHE was previously studied in spinless cold fermion models [16], which are very hard to be achieved in the realistic experiments, we have proposed here a novel scheme to observe QAHE in spin-1/2 fermion system which is truly accessible with current experimental platforms.

Chiral topological superfluid phase.—We next study the topological chiral superfluid phase by considering an s-wave interaction which can be well controlled with Feshbach resonance in cold atoms [29]. In optical lattice, this interaction is described by the attractive Fermi Hubbard model $H_{\rm int} = -\sum_{\vec{i}} U n_{\vec{i}\uparrow} n_{\vec{i}\downarrow}$, where the regularized 2D effective interaction $U = \hbar^2 a_s \sqrt{8\pi}/(m l_z l_{\rm 2d}^2)$ with $l_z = (h/m\omega_z)^{1/2}$, $l_{\rm 2d} = (h/m\omega_{\rm 2d})^{1/2}$, and the s-wave scattering length $a_s > 0$. The parameters ω_{2d} and ω_z denote the 2D square lattice trapping frequency and a tight trapping frequency along z axis, respectively. We first study the superfluid phase with the self-consistent mean field approach by introducing the s-wave superfluid order parameter by $\Delta_s = (U/N_0)\sum_{\mathbf{k}} \langle c_{\mathbf{k}\uparrow} c_{-\mathbf{k}\downarrow}\rangle$ with N_0 the number of lattice sites. Then the total Hamiltonian in the Nambu basis $\psi_{\mathbf{k}} = (c_{\mathbf{k}\uparrow}, c_{\mathbf{k}\downarrow}, c^\dagger_{-\mathbf{k}\downarrow}, -c^\dagger_{-\mathbf{k}\uparrow})$ can be written as $H_{\rm BdG} = \sum_{\mathbf{k}} \psi^\dagger_{\mathbf{k}} \mathcal{H}_{\rm BdG}(\mathbf{k}) \psi_{\mathbf{k}}$, where

$$\begin{aligned} \mathcal{H}_{\rm BdG} &= d_x \sigma_x \otimes \tau_z + d_y \sigma_y \otimes \tau_z + d_z \sigma_z \otimes I - \mu I \otimes \tau_z + \\ &\quad + (\Delta_s I \otimes \tau_+ + \text{H.c.}). \end{aligned} \quad (4)$$

Here μ is the chemical potential, $\tau_{x,y,z}$ are Pauli matrices acting on the Nambu space, and $\tau_\pm = (\tau_x \pm i\tau_y)/2$. The s-wave order parameter is solved by the gap equation

$$\frac{N_0}{U} = \frac{1}{4}\sum_{\mathbf{k},\alpha=\pm} \frac{1}{E_{\mathbf{k}}^\alpha}\left[1 + \alpha \frac{d_z^2(\mathbf{k})}{w_{\mathbf{k}}}\right] \tanh\left(\frac{1}{2}\beta E_{\mathbf{k}}^\alpha\right), \quad (5)$$

where the energy spectra $E_{\mathbf{k}}^\pm = (\Gamma^2 + |\vec{d}_{\mathbf{k}}|^2 \pm 2w_{\mathbf{k}})^{1/2}$ by diagonalizing $\mathcal{H}_{\rm BdG}$, with $w_{\mathbf{k}} = [\mu^2(d_x^2 + d_y^2) + d_z^2\Gamma^2]^{1/2}$ and $\Gamma^2 = \mu^2 + |\Delta_s|^2$, and $\beta = 1/(k_B T)$.

To identify an effective $p + ip$ chiral superfluid phase from the Hamiltonian $\mathcal{H}_{\rm BdG}$, we analyze the special situation with $m_z = 4t_s$. In this case the low energy spectrum is captured by the Hamiltonian (up to linear order of the momentum) $\mathcal{H}_{\rm BdG} = 2t_{\rm so}^{(0)}(k_x\sigma_y + k_y\sigma_x)\tau_z - \mu\tau_z + (\Delta_s\tau_+ + \text{H.c.})$. It is interesting that this low-energy model is equivalent to the surface Hamiltonian of a 3D topological insulator in proximity to an s-wave SC [4], which renders the 2D chiral $p + ip$ topological SC phase. We therefore expect that in our model the chiral Majorana edge modes and MZM in the vortex core can be obtained. Similar as the case in QAHE, the SF phase diagram can also be determined by analyzing the properties of the bulk gap. By examining $E_{\mathbf{k}}^-$ with $m_z > 0$ we find that the bulk gap closes at $\mathbf{k} = (0,0)$ and $\mathbf{k} = (\pi,\pi)$ for $\mu^2 + |\Delta_s|^2 = (m_z - 4t_s)^2$ and $(m_z + 4t_s)^2$, respectively. Furthermore, at the points $\mathbf{k} = (0,\pi)$ and $\mathbf{k} = (\pi,0)$ the bulk gap closes if $\mu^2 + |\Delta_s|^2 = m_z^2$. These properties lead to a rich phase diagram as presented below. From the low-energy Hamiltonian $\mathcal{H}_{\rm BdG}$ we know that the superfluid phase with $|\Delta_s| \gtrsim 0$, $m_z = 4t_s$, and $\mu = 0$ is topological. This implies that if $|m_z| > 2t_s$, the SF phase is topologically nontrivial with Chern number $C_1^{\rm SF} = +1$ for $(|m_z| - 4t_s)^2 < \mu^2 + |\Delta_s|^2 < m_z^2$, and $C_1^{\rm SF} = -1$ for $m_z^2 < \mu^2 + |\Delta_s|^2 < (|m_z| + 4t_s)^2$. The change by 2 in the Chern number is originated from the fact that tuning $\mu^2 + |\Delta_s|^2$ from less than to larger than m_z^2 reverses the mass terms at both $\mathbf{k} = (0,\pi)$ and $\mathbf{k} = (\pi,0)$. On the other hand, when $m_z = 0$ the phase is always trivial. Actually, when $m_z = 0$ the low-energy Hamiltonian $\mathcal{H}_{\rm BdG}$ for the SF is captured by two Dirac cones around $\mathbf{k} = (0,\pi)$ and $\mathbf{k} = (\pi,0)$ with opposite chiralities and having s-wave pairing. Such two Dirac cones resemble $p + ip$ and $p - ip$ superfluids, respectively, which couple to each other and cancel out, yielding a trivial phase. With this result we know that if $|m_z| < 2t_s$, the SF phase is topologically trivial for $m_z^2 < \mu^2 + |\Delta_s|^2 < (|m_z| - 4t_s)^2$, while it is nontrivial with $C_1^{\rm SF} = -1$ when $(|m_z| - 4t_s)^2 < \mu^2 + |\Delta_s|^2 < |m_z| + 4t_s)^2$. In cold atoms the parameters such as m_z, t_s and μ can be precisely adjusted in the experiment to tune the system into topological chiral SF phases.

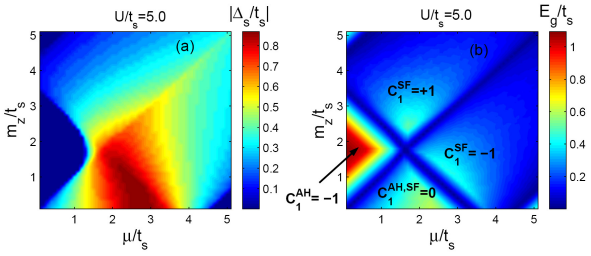

FIG. 2: (Color online) Self-consistent calculations of the s-wave order Δ_s [for (a)] and the bulk gap E_g [for (b)] versus m_z and μ at zero temperature. Topological phase transition occurs at $E_g = 0$. The hopping coefficients $t_{\rm so}^{(0)} = t_s$.

The self-consistent solutions for Δ_s and mean-field phase diagram are shown in Fig. 2 (a) and (b), respectively. It can be seen that the s-wave order Δ_s vanishes when the noninteracting Hamiltonian $H_{\rm TI}$ has a large insulating gap and the chemical potential μ locates deep in the band gap [left most area in (a)]. On the other

hand, an appreciable Δ_s is obtained in the area with $1.5t_s < \mu < 3.5t_s$ and $0 < m_z < 3.0$. In such parameter regime the SO terms of d_x and d_y dominates over d_z and a relatively large density of states at Fermi level is present. In Fig. 2 (b) the superfluid phases with both $C_1^{\rm SF} = +1$ and -1 are obtained, respectively leading to chiral and anti-chiral Majorana edge modes localized in the boundary [1].

Note that in 2D superfluids no long-range order exists at finite temperature and the critical temperature by mean-field theory is often overestimated. Instead, the Berezinsky-Kosterlitz-Thouless (BKT) transition occurs at the critical temperature which is limited by entropically driven vortex and antivortex proliferation [30]. The BKT temperature is calculated by

$$T_{\rm BKT} = \frac{\pi}{2}\rho_s(\Delta_s, T_{\rm BKT}), \tag{6}$$

where ρ_s is the superfluid stiffness (superfluid density). With the presence of phase fluctuation, the superfluid order parameter can be described by $\Delta_s = \Delta_0 e^{i\theta(\mathbf{r})}$, where θ varies slowly in the position space. The simplest way to estimate the stiffness is to use its relation to the supercurrent density $\mathbf{j}_s = \rho_s \nabla\theta(\mathbf{r})$. For the case that θ varies slowly with position, we can approximate that $\mathbf{q} = \nabla\theta(\mathbf{r})$, which implies that the s-wave pairing occurs between two fermions with a center-of-mass momentum $\mathbf{q}$. The current of the system can also be calculated by $\mathbf{j}_s = \frac{1}{A}{\rm Tr}[e^{-\beta H_{\rm BdG}}\partial H_{\rm BdG}(\mu,\Delta_0,\nabla\theta)/\partial\mathbf{q}]/{\rm Tr}[e^{-\beta H_{\rm BdG}}]$, with A the area of the square lattice. This leads to

$$\rho_s = \frac{1}{\mathbf{q}A}\frac{{\rm Tr}\left[e^{-\beta H_{\rm BdG}}\partial^2 H_{\rm BdG}(\mu,\Delta_0,\nabla\theta)/\partial(\nabla\theta)^2\right]}{{\rm Tr}[e^{-\beta H_{\rm BdG}}]}. \tag{7}$$

Together with the gap equation for Δ_s we get the superfluid stiffness. It can be verified that the above results are consistent with those through a standard functional path integral approach, where the phase fluctuation of the superfluid order parameter is described by an effective action $S_{\rm fluc} = (1/2)\int d^2\mathbf{r}\rho_s(\nabla\theta)^2$. The BKT temperature is then given by Eq. (6). We have numerically confirmed that when $\Delta_s = 0$ the supercurrent $\mathbf{j}_s$ vanishes.

The numerical results for $T_{\rm BKT}$ versus U and μ are shown in Fig. 3. For the case that the Fermi energy touches the bulk edge, the BKT temperature increases gradually with U [blue line in Fig. 3(a)], while when the Fermi energy locates deep into the bulk, the critical temperature increases sharply with U and approaches a saturate magnitude in a small Hubbard interaction (red, green, and black curves). The BKT temperature versus μ with fixed $U = 5t_s$ and m_z is plotted in Fig. 3(b). It can be found that with $m_z = 3t_s$, the maximum $T_{\rm BKT}$ is around $0.3t_s$. Note that the upper value of the blue detuning is limited by the hyperfine-structure splitting and can be taken as $2\pi \times 1.7$THz for ^{40}K atoms, which gives the recoil energy $E_R/\hbar \sim \hbar k_0^2/2m = 2\pi \times 8.5$kHz using lasers of wavelength 764nm to form the square lattice.

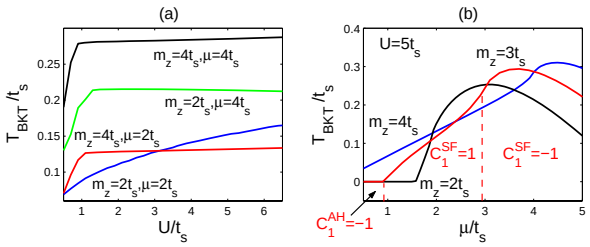

FIG. 3: (Color online) BKT temperature as a function of U with different values of m_z and μ (a), and versus μ at $U = 5t_s$ and with different magnitudes of m_z (b). The SO coupled hopping $t_{\rm so}^{(0)} = t_s$. Topological orders of different Chern numbers are indicated for the case with $m_z = 3t_s$.

Taking that $\Omega_0 = 2\pi \times 0.27$GHz, we have $V_0 = 5E_R$, the lattice trapping frequency $\omega = 2\pi \times 34.9$kHz, and the hopping coefficients $t_{\rm so}^{(0)}/\hbar \sim t_s/\hbar \simeq 2\pi \times 0.52$kHz. With this parameter regime we find that the bulk gap for QAHE $E_g = 2\pi \times 1.04$kHz by setting $\delta = 2t_s$, corresponding to the temperature $T = 90$nK for observation, and the maximum BKT temperature for the topological superfluid phase with $U = 5t_s$ is about 10nK.

Conclusions and Discussions.—We have proposed a truly experimental scheme to observe 2D SO interaction which leads to both the quantum anomalous Hall effect and chiral topological superfluid phase in spin-1/2 cold fermions trapped with a blue-detuned square optical lattice and coupled to two periodic Raman fields. We calculated the bulk gap of the topological states and the BKT temperature of the topological superfluid phase, and show that the predicted topological orders are reachable with the realistic parameter regimes.

The present model exhibits many essential advantages in the realization. First of all, the square optical lattice and the Raman fields, used to induce 2D SO interactions, are generated simultaneously through the same laser fields, which greatly simplifies the setup for experimental studies. On the other hand, for blue-detuned optical lattice the atoms are trapped in the minimums of lattice potentials which may generally minimize heating effects [31]. Note that while the topological superfluid phase with Majorana modes requires a fermion system, the topological insulating state can be demonstrated with cold bosons [32], which makes experimental observations even more straightforward. It is worthwhile to point out that 2D chiral topological orders are classified by a Z invariant, and is stable when stacking multi-layers of the 2D system. This enables a study of topological superfluids in the multi-layer square lattices which may have a higher transition temperature. The present work paves the way to observe 2D topological orders in cold atoms, and will lead to the ultimate observation of non-Abelian Majorana fermions with realistic cold atom platforms.

We appreciate Gyu-boong Jo much for very helpful discussions on the experimental feasibility of this work.

We also thank H. Zhai, M. Cheng, Patrick A. Lee, Wujie Huang, C. Wu, and Z.-X. Liu for useful discussions. We acknowledge the support from HKRGC through Grant 605512 and HKUST3/CRF09.

[1] N. Read and D. Green, Phys. Rev. B **61**, 10267 (2000); A. Kitaev, Physics-Uspekhi **44**, 131 (2001).
[2] D. A. Ivanov, Phys. Rev. Lett. **86**, 268 (2001); J. Alicea, Y. Oreg, G. Refael, F. von Oppen, and M. R. A. Fisher, Nature Phys. **7**, 412 (2011).
[3] S. Das Sarma, M. Freedman, and C. Nayak, Phys. Rev. Lett. **94**, 166802 (2005).
[4] L. Fu and C. L. Kane, Phys. Rev. Lett. **100**, 096407 (2008); X.-L. Qi, T. L. Hughes, and S. -C. Zhang, Phys. Rev. B **82**, 184516 (2010).
[5] J. D. Sau, R. M. Lutchyn, S. Tewari, and S. D. Sarma, Phys. Rev. Lett. **104**, 040502 (2010).
[6] R. M. Lutchyn, J. D. Sau, and S. D. Sarma, Phys. Rev. Lett. **105**, 077001 (2010); Y. Oreg, G. Refael, and F. von Oppen, *ibid* **105**, 177002 (2010); A. C. Potter and P. A. Lee, *ibid* **105**, 227003 (2010).
[7] V. Mourik, K. Zuo, S. M. Frolov, S. R. Plissard, E. P. A. M. Bakkers, and L. P. Kouwenhoven, **336**, 1003 (2012); M. T. Deng, M. T. *et al.,* arXiv:1204.4130v1 (2012); A. Das, *et al.,* Nature Phys. **8**, 887 (2012).
[8] K. T. Law, P. A. Lee, and T. K. Ng, Phys. Rev. Lett. **103**, 237001 (2009); K. Flensberg, Phys. Rev. B **82**, 180516(R) (2010). X. -J. Liu, and A. M. Lobos, *ibid* **87**, 060504(R) (2013).
[9] X. -J. Liu, M. F. Borunda, X. Liu, and J. Sinova, Phys. Rev. Lett. **102**, 046402 (2009).
[10] Y.-J. Lin, K. Jiménez-García, and I. B. Spielman, Nature **471**, 83 (2011).
[11] M. Chapman and C. Sá de Melo, Nature **471**, 41 (2011).
[12] P. Wang, Z.-Q. Yu, Z. Fu, J. Miao, L. Huang, S. Chai, H. Zhai, and J. Zhang, Phys. Rev. Lett. **109**, 095301 (2012).
[13] L. W. Cheuk, A. T. Sommer, Z. Hadzibabic, T. Yefsah, W. S. Bakr, and M. W. Zwierlein, Phys. Rev. Lett. **109**, 095302 (2012).
[14] J. -Y. Zhang et al., Phys. Rev. Lett. **109**, 115301 (2012).
[15] X. -J. Liu, X. Liu, L. C. Kwek and C. H. Oh, Phys. Rev. Lett. **98**, 026602 (2007); Phys. Rev. B **79**, 165301 (2009).
[16] C. Wu, Phys. Rev. Lett. **101**, 186807 (2008); X.-J. Liu, X. Liu, C. Wu, and J. Sinova, Phys. Rev. A **81**, 033622 (2010); M. Zhang, H. -h. Hung, C. Zhang, and C. Wu, *ibid* **83**, 023615 (2011). N. Goldman, J. Beugnon, and F. Gerbier, Phys. Rev. Lett. **108**, 255303 (2012). S. -S. Zhang, H. Fan, and W. -M. Liu, Phys. Rev. A **87**, 023622 (2013).
[17] N. Goldman, I. Satija, P. Nikolic, A. Bermudez, M.A. Martin-Delgado, M. Lewenstein, I. B. Spielman, Phys. Rev. Lett. **105**, 255302 (2010); N. Goldman, J. Beugnon, and F. Gerbier, *ibid* **108**, 255303 (2012).
[18] L. -J. Lang, X. Cai, and S. Chen, Phys. Rev. Lett. **108**, 220401 (2012).
[19] X. -J. Liu, Z. -X. Liu, and M. Cheng, Phys. Rev. Lett. **110**, 076401 (2013); X. Li, E. Zhao, and W. V. Liu, Nature Comm. **4**, 1523 (2013).
[20] C. Zhang, S. Tewari, R. Lutchyn, and S. Das Sarma, Phys. Rev. Lett. **101**, 160401 (2008); Y. Zhang, L. Mao, C. Zhang, *ibid* **108**, 035302 (2012).
[21] M. Sato, Y. Takahashi, S. Fujimoto, Phys. Rev. Lett. 103 020401 (2009); S. -L. Zhu, L. B. Shao, Z. D. Wang, L. -M. Duan, *ibid* **106**, 100404 (2011).
[22] J. D. Sau, R. Sensarma, S. Powell, I. B. Spielman, and S. Das Sarma, Phys. Rev. B **83**, 140510(R) (2011).
[23] X. -J. Liu and P. D. Drummond, Phys. Rev. A **86**, 035602 (2012); R. Wei and E. J. Mueller, *ibid* **86**, 063604 (2012); X. -J. Liu, *ibid* **87**, 013622 (2013).
[24] W. Yi and G.-C. Guo, Phys. Rev. A **84**, 031608(R) (2011); L. He, X. -G. Huang, Phys. Rev. Lett. **108**, 145302 (2012); F. Wu, G. -C. Guo, W. Zhang, and W. Yi, *ibid* **110**, 110401 (2013).
[25] Z. -Q. Yu and H. Zhai, Phys. Rev. Lett. **107**, 195305 (2011); H. Hu L. Jiang, X.-J. Liu, and H. Pu, *ibid* **107**, 195304 (2011); L. Dell'Anna, G. Mazzarella, and L. Salasnich, Phys. Rev. A **86**, 053632 (2012).
[26] Y. Li, L. P. Pitaevskii, and S. Stringari, Phys. Rev. Lett. **108**, 225301 (2012). K. Seo, L. Han, and C. A. R. Sá de Melo, *ibid* **109**, 105303 (2012).
[27] D.-W. Zhang, Z.-Y. Xue, H. Yan, Z. D. Wang, S.-L. Zhu, Phys. Rev. A **85**, 013628 (2012); M. -Y. Ye and X. -M. Lin, arXiv:1207.5369v1 (2012).
[28] V. Galitski and I. B. Spielman, Nature **494**, 49 (2013). X. Zhou, Y. Li, Z. Cai, and C. Wu, arXiv:1301.5403v1 (2013).
[29] I. Bloch, J. Dalibard, and W. Zwerger, Rev. Mod. Phys. **80**, 885 (2008).
[30] V. L. Berezinskii, Sov. Phys. JETP **32**, 493 (1971); J. M. Kosterlitz and D. Thouless, J. Phys. **C5**, L124 (1972).
[31] R. Ozeri, L. Khaykovich, and N. Davidson, Phys. Rev. A **59**, 1750(R)(1999); F. Gerbier and Y. Castin, *ibid* **82**, 013615 (2010); M. Takamoto, H. Katori, S. I. Marmo, V. D. Ovsiannikov, and V. G. Pal'chikov, Phys. Rev. Lett. **102**, 063002 (2009).
[32] M. Atala et al., arXiv:1212.0572v1 (2012).